The flux of small near-Earth objects colliding with the Earth

P. Brown*†, R. E. Spalding‡, D. O. ReVelle†, E. Tagliaferri§ & S. P. Worden‖

** Department of Physics and Astronomy, University of Western Ontario, London, Ontario N6A 3K7, Canada*
‡ Sandia National Laboratory, Org. 5740, MS 0973, PO Box 5800, Albuquerque, New Mexico 87185, USA
† Los Alamos National Laboratory, PO Box 1663, MS J577, Los Alamos, New Mexico 87545, USA
§ ET Space Systems, 5990 Worth Way, Camarillo, California 93012, USA
‖ Directorate of Operations, United States Space Command, Peterson Air Force Base, Colorado Springs, Colorado 80914-3190, USA

Asteroids with diameters smaller than ~50-100 m that collide with the Earth usually do not hit the ground as a single body; rather, they detonate in the atmosphere[1]. These small objects can still cause considerable damage, such as occurred near Tunguska[2], Siberia, in 1908. The flux of small bodies is poorly constrained, however, in part because ground-based observational searches pursue strategies that lead them preferentially to find larger objects[3]. A Tunguska-class event—the energy of which we take to be equivalent to 10 megatons of TNT—was previously estimated to occur every 200–300 years, with the largest annual airburst calculated to be ~20 kilotons (kton) TNT equivalent (ref. 4). Here we report satellite records of bolide detonations in the atmosphere over the past 8.5 years. We find that the flux of objects in the 1–10-m size range has the same power-law distribution as bodies with diameters >50 m. From this we estimate that the Earth is hit on average annually by an object with ~5 kton equivalent energy, and that Tunguska-like events occur about once every 1,000 years.

Our data are based on observations made by United States Department of Defense and Department of Energy space-based systems in geostationary orbits. These systems are designed to detect the signature of nuclear explosions and other objects of military interest on or above Earth's surface[5]. For the past eight years, data from optical events registered as probable bolides have been recorded and saved for later examination. In total, 300 events from February 1994 to September 2002 have been designated as probable bolides, and a time–intensity plot for each event recorded. From these time–intensity plots, the peak radiated power (maximum brightness) and the integrated energy were determined. Figure 1 shows an example of the original data for a large bolide recorded on 6 June 2002.

From this data set of recorded optical flashes, we obtain a number distribution of the optical energies of the 300 bolides in our sample. The total optical energy is expected to be an indicator of the original kinetic energy of the meteoroid[6]. We corrected the number distribution based on the percentage coverage of the Earth's surface, which varied from 60% to 80% throughout the period of study.

To convert these raw optical energy estimates to an equivalent source energy requires knowledge of several poorly known parameters. First, the spectral energy distribution at the source needs to be defined to determine the true radiated energy detected by the sensor. This process requires knowledge of the spectrum of the bolide. Previous workers have assumed a 6,000 K blackbody distribution[5], but the dominant line emission from bright fireballs observed from the ground suggests that this assumed distribution might be a poor approximation[7]. In the absence of better data for these larger fireballs, we continue for consistency to use the 6,000 K blackbody assumption as others have also done[8]. As the peak in sensitivity for the optical sensors is near this temperature, our corrections to the energy estimates will be more conservative than would be the case if the fireball temperatures were closer to 4,500 K (ref. 9). We expect the 6,000 K temperature assumption to produce less than ~30% uncertainty on the final flux numbers.

Second, a much greater unknown is establishing the fraction of total initial kinetic energy transformed into light production. This integral luminous efficiency (τ_I; ref. 10) has been measured to be of the order 3% for photographically measured fireballs with energies between 10^{-5} and 10^{-1} kton (median of the sample, 7×10^{-4} kton)[7]. Theoretical models[8] suggest that this value should be 10–15% for bolides of chondritic composition with energies between 10^{-1} and 10 kt, with the efficiency increasing as energy increases. More generally, we expect that the integral efficiency will be a complex function of velocity, mass, entry angle, body shape and composition, as well as porosity[11], differing from one bolide to the next. This effect is reflected in the wide variability observed in the analysis of high-precision ground-based bolide data where an order-of-magnitude, systematic variation in luminous efficiency between strong/chondritic bodies (highest values) to weak bodies (lowest) is found[12]. No observational constraints for this value as a function of energy have been previously published for objects in our size range.

In an attempt to derive an empirical fit for τ_I for our population, we have examined those fireball events recorded by optical sensors and for which an independent estimate of the energy exists. A total of 13 events have optical data and independent energy estimates (Table 1).

The fit between optical energy and total calibrated energy (Fig. 2) leads to:

$$\tau_I = (0.1212 \pm 0.0043) E_o^{0.115 \pm 0.075} \quad (1)$$

where E_o is the optical energy (in kilotons TNT equivalent, 4.185×10^{12} J) measured by the space-based sensors assuming a 6,000 K blackbody emission from the bolides.

Applying this form of the integral luminous efficiency under our 6,000 K blackbody assumption to the bolide data set collected over 8.5 years, we find the flux as a function of impact energy (Fig. 3; see figure legend for details). We also convert these total impact energies into equivalent diameter of colliding body, assuming a mean impact velocity with the Earth of 20.3 km s^{-1} (W. Bottke, personal communication) and a bulk density of 3,000 kg m^{-3}, an appropriate compromise between ordinary chondritic densities (average near 3,400 kg m^{-3}) and primitive (CI/CM) carbonaceous chondrite densities (average near 2,600 kg m^{-3})[13]. We note that below ~10^{-1} kton, a roll-off in the cumulative number of bolides detected by the satellite is observed as the system limiting sensitivity is approached.

The power-law fit to the satellite data shown in Fig. 3 can also be

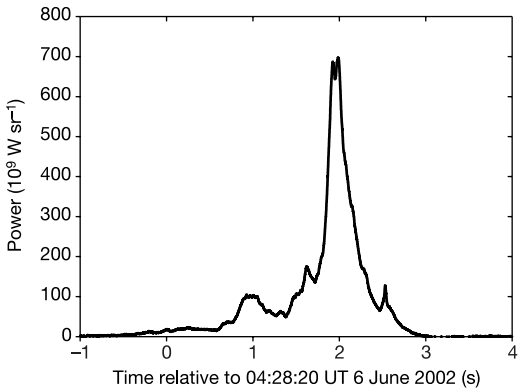

Figure 1 Optical light curve from the 6 June 2002 bolide over the Mediterranean Sea. The estimated energy for this event (on the basis of infrasonic/acoustic data) was 26 kton TNT equivalent.

Table 1 **Details of calibrated bolides shown in Fig. 2**

Bolide date	Time (UT)	Location (lat., long.)	Optical energy (kt)	Calibrated energy (kt)	Calibration method*
25/7/02	15:58	29° S, 47° E	0.060	0.60 ± 0.20	Infrasound
6/6/02	04:28	34°N, 21°E	0.908	25.77 ± 2.16	Infrasound
9/3/02	01:20	7°N, 147°W	0.053	1.05 ± 0.79	Infrasound
23/4/01	06:12	28°N, 134°W	1.100	0.63 ± 0.33	Infrasound
25/8/00	01:12	15°N, 106°W	0.337	2.35 ± 1.24	Infrasound
6/5/00	11:52	50°N, 18°E	0.006	0.09 ± 0.04	Infrasound/meteorites[22]
18/2/00	09:26	1°S, 109°E	0.860	3.89 ± 0.73	Infrasound
18/1/00	16:43	60°N, 135°W	0.263	1.66 ± 0.70	Infrasound/velocity/meteorites[23]
16/8/99	05:18	35°N, 107°W	0.009	0.18 ± 0.03	Infrasound
9/10/97	18:47	32°N, 106°W	0.045	0.29	Infrasound[24]
15/6/94	00:03	46°N, 73°W	0.003	0.03 ± 0.01	Meteorites/velocity[25]
7/5/91	23:04	50°N, 15°E	0.012	0.19	Photos/spectra/ velocity[26]
-		-	0.0007	0.0164	Photos/velocity[9]

*Calibration methods include: 'infrasound', infrasound energy derived from period at maximum amplitude[20]; 'meteorites', recovery mass estimate from cosmogenic nuclides; 'velocity', entry velocity and trajectory known; 'photos', multi-station photos of fireball; and 'spectra', spectral records of fireball. The final row of data represents the median values of the fireball events given in ref. 8.

represented by an equation of the form

$$\log N = a_0 - b_0 \log E \quad (2)$$

where N is the cumulative number of objects colliding with the Earth each year with energies of E (in kilotons) or greater; in this representation, $a_0 = 0.5677 \pm 0.015$, and $b_0 = 0.90 \pm 0.03$. We may recast this in terms of diameter of the colliding body using our assumptions above as:

$$\log N = c_0 - d_0 \log D \quad (3)$$

where D is the meteoroid diameter in metres, $c_0 = 1.568 \pm 0.03$, and $d_0 = 2.70 \pm 0.08$.

Comparing our result to debiased Lincoln Near Earth Asteroid Research (LINEAR) measurements[14] as shown in Fig. 3, we see that our power-law determination is in good agreement (within error) with the flux values estimated based on the small number (~30) of tens-of-metres class LINEAR discoveries. Influx estimates based on lunar crater[15] counts extend down to meteoroids of several metres

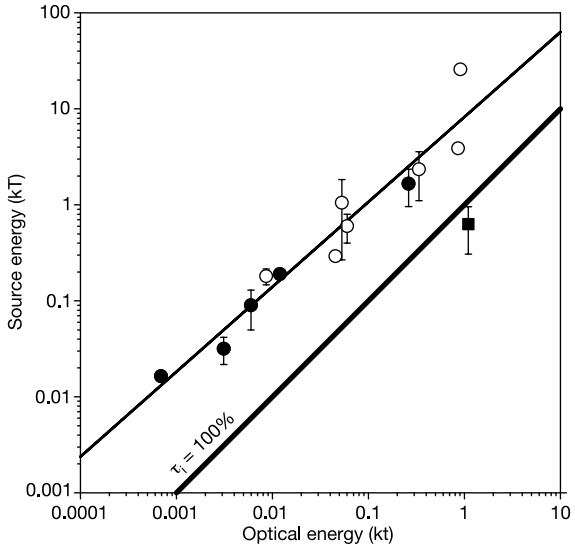

Figure 2 Bolide energy calibrations. These are based on simultaneous observations by optical sensors (or equivalent) and energy estimated from another technique. The optical energy estimates are made assuming a 6,000 K blackbody. Open circles, events that have also been detected infrasonic/acoustically and for which a source energy was computed using the calibrated relation between energy and period at maximum signal amplitude[20]. Only events with periods greater than two seconds were used, to avoid issues of Doppler wind changes at small signal periods. Filled circles, events that have higher-precision source energy calibrations owing to recovery of meteorites and/or availability of information on atmospheric velocity—see Table 1 for details. The filled square represents the 23 April 2001 fireball event, which is particularly unusual[27] and was excluded from our analysis. The upper solid line shows the fit to the data represented by open and filled circles. The lower, thicker, solid line represents objects with integral luminous efficiencies of 100%; that is, those bodies to the right of this curve are unphysical within the context of our assumptions.

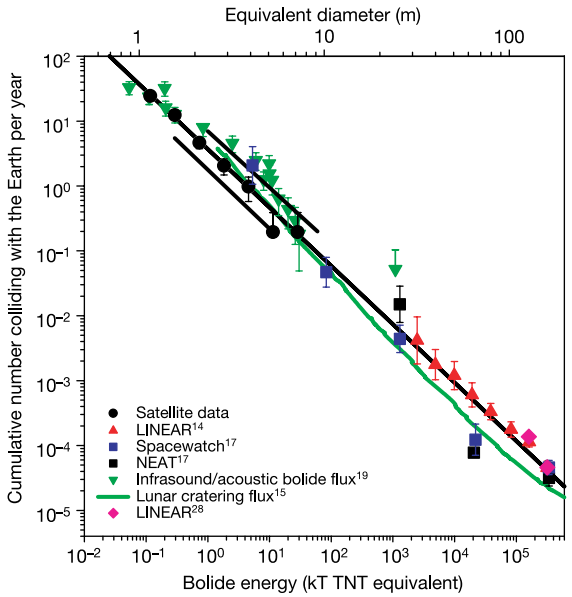

Figure 3 The flux of small near-Earth objects colliding with the Earth, for diameters less than 200 m. Filled circles, the satellite-determined flux based on 8.5 years of global observations (this work). The black best-fit line represents data for objects in excess of ~1 m in diameter where optical sensor data are most complete. Error bars represent counting statistics only. The thick black lines above and below the satellite flux represent the extreme limits, assuming integral luminous efficiencies for the entire population of 5% (top line) and 20% (bottom line). On the basis of the fit in Fig. 2 over our energy range of interest, τ_I varies from 6% to15%. From ground-truth calibrations and the analysis summarized in Fig. 2, we adopt 5% and 20% as the extreme probable limits for the average integral luminous efficiencies over the energy range represented by the lines. For comparison, we plot debiased estimates of the near-Earth asteroid impact frequency based on telescopic search data for smaller LINEAR discoveries (upward red triangles)[14] and larger LINEAR discoveries[28](pink diamonds), Near-Earth Asteroid Tracking (NEAT) (filled squares) and Spacewatch (blue squares)[17] surveys, where diameters are determined assuming an albedo of 0.1. LINEAR values at the smaller sizes are normalized to the larger LINEAR discoveries[28]. Energy for telescopic data is computed assuming a mean bulk density of 3,000 kg m^{-3} and an average impact velocity of 20.3 km s^{-1}. The intrinsic impact frequency for these telescopic data was found by computing the average probability of impact for the 1,000 largest known near-Earth asteroids, and using this frequency (2×10^{-9} yr^{-1}) as the average for the entire population[14]. As well, the infrasonic/acoustically measured bolide flux (downward dark green triangles)[19] and lunar crater counts assuming a geometric albedo of 0.25 (solid green line)[15] are shown.

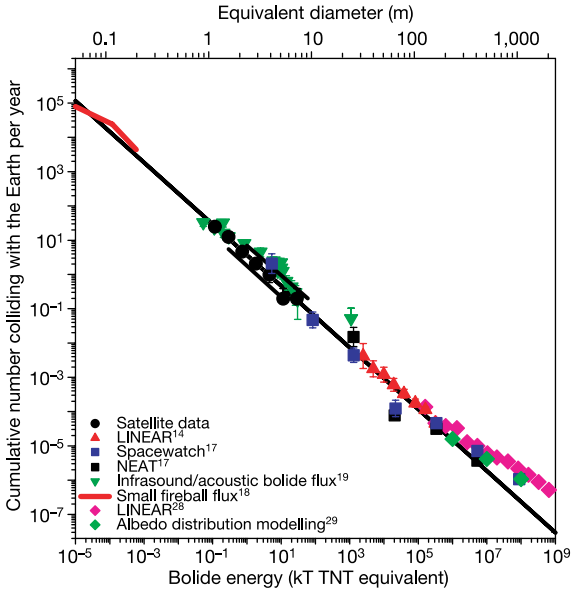

Figure 4 The flux of small near-Earth objects colliding with the Earth. Data are shown over a range of 14 magnitudes of energy. In addition to data shown in Fig. 3, this plot also shows the Earth collision hazard in the 1,000 Mton and larger energy range, based on modelling the albedo distribution of near-Earth asteroids[29]. At smaller sizes, the power-law number distribution derived from a decade-long survey of ground-based observations of fireballs[18] is indicated.

diameter, and we find a good fit with these data in the 3–10-m size range assuming an average geometric albedo of 0.25. We are unable to match the crater flux curve over the 3–10-m size range with our data for a typical main-belt mean albedo of 0.11 (near the average for C and S types in the main belt), further supporting the notion that small near-Earth asteroids have higher mean albedos than large main-belt asteroids[16]. We note, however, that the true geometric albedo distribution for the near-Earth asteroid population is uncertain.

The only telescopic flux measurement to overlap our population directly is that based on a debiasing of Spacewatch data[17]. In particular, the Spacewatch estimate (albeit with large error) of the flux of 4- and 10-m diameter bodies striking the Earth is in agreement with our satellite energy estimates within error limits.

We also find that extrapolation of our power law is in agreement with the flux of smaller bodies[18] for energies between 10^{-5} kton and 10^{-3} kton (Fig. 4), these data being based on observations with ground-based cameras of fireballs having energies of $<10^{-3}$ kton. However, the influx measurements derived from infrasonic/acoustic measurements are slightly higher on average than the satellite estimates (notably between 1 kton and 10 kton), though in agreement near the upper end of our energy range where the infrasonic/acoustic set has the best overall global coverage. One possible reason for the difference is the small number of statistics associated with the infrasound/acoustic data (only 19 events in total). Alternatively, a large range in meteoroid porosity may influence the optical light curve interpretation, potentially making an order-of-magnitude difference between the estimated and true energy. That the infrasonic/acoustic and satellite influx agree in the size range in which both are accurate (~7–10 m) is further evidence that the most of the flux of bodies striking the Earth is asteroidal, rather than cometary, as only deeply penetrating bodies can generate infrasonic/acoustic shocks and thus be detected with these infrasonic/acoustic systems[19,20]. Agreement in fit between our power-law extrapolation (solid line in Fig. 3) and LINEAR data, as well as with the cratering record and infrasonic/acoustic data at larger sizes, further suggests that objects of cometary origin make a small contribution to the flux of 1–10-m bodies striking the Earth[21].

Using the best fit of these satellite data and extrapolating the power law to higher energies, we find that the Earth is struck by an object with the energy of Tunguska (assumed to be 10 MT) every $1{,}000^{+800}_{-200}$ years (with an allowed range from 400 to 1,800 years on the basis of our most extreme assumptions for luminous efficiency). We estimate that the Earth is on average struck annually by an object of energy ~5 kton (with a possible range of 2–10 kton), and struck each month by an object with 0.3 kt of energy. Every ten years, an object of energy ~50 kton impacts Earth. □

Received 9 October; accepted 21 October 2002; doi:10.1038/nature01238.

1. Hills, J. G. & Goda, P. Damage from the impacts of small asteroids. *Planet. Space Sci.* **46,** 219–229 (1998).
2. Sekanina, Z. Evidence for the asteroidal origin of the Tunguska object. *Planet. Space Sci.* **46,** 191–204 (1998).
3. Morrison, D., Chapman, C. R. & Slovic, P. *Hazards due to Comets and Asteroids* (ed. Gehrels, T.) 59–91 (Univ. Arizona Press, Tucson, 1994).
4. Shoemaker, E. M. Asteroid and comet bombardment of the Earth. *Annu. Rev. Earth Planet. Sci.* **11,** 461–494 (1983).
5. Tagliaferri, E., Spalding, R., Jacobs, C., Worden, S. P. & Erlich, A. *Hazards due to Comets and Asteroids* (ed. Gehrels, T.) 199–221 (Univ. Arizona Press, Tucson, 1994).
6. McCord, T. B. *et al.* Detection of a meteoroid entry into the Earth's atmosphere on February 1, 1994. *J. Geophys. Res.* **100,** 3245–3249 (1995).
7. Ceplecha, Z. *et al.* Meteor phenomena and bodies. *Space Sci. Res.* **84,** 327–471 (1998).
8. Nemtchinov, I. *et al.* Assessment of kinetic energy of meteoroids detected by satellite-based light sensors. *Icarus* **130,** 259–274 (1997).
9. Ceplecha, Z., Spalding, R. E., Jacobs, C. & Tagliaferri, E. *Proc. SPIE* **2813,** 46–56 (1996).
10. ReVelle, D. O. A predictive macroscopic integral radiation efficiency model. *J. Geophys. Res.* **85,** 1803–1808 (1980).
11. ReVelle, D. O. *Meteoroids 2001—Conference Proceedings* SP-495 (ed. Warmbein, B.) 513–519 (European Space Agency, Noordijuk, The Netherlands, 2001).
12. ReVelle, D. O. & Ceplecha, Z. *Meteoroids 2001—Conference Proceedings* SP-495 (ed. Warmbein, B.) 507–512 (European Space Agency, Noordijuk, The Netherlands, 2001).
13. Britt, D. & Consolmagno, G. The porosity of dark meteorites and the structure of low-albedo asteroids. *Icarus* **146,** 213–219 (2000).
14. Harris, A. W. in *Proc. Asteroids, Comets, Meteors 2002*, (Berlin, in the press).
15. Werner, S. C., Harris, A. W., Neukum, G. & Ivanov, B. A. NOTE: The near-Earth asteroid size-frequency distribution: a snapshot of the lunar impactor size-frequency distribution. *Icarus* **156,** 287–290 (2002).
16. Harris, A. W. & Davies, J. K. Physical characteristics of near-Earth asteroids from thermal infrared spectrophotometry. *Icarus* **142,** 464–475 (1999).
17. Rabinowitz, D., Helin, E., Lawrence, K. & Pravdo, S. A reduced estimate of the number of kilometre-sized near-Earth asteroids. *Nature* **403,** 165–166 (2000).
18. Halliday, I., Griffin, A. A. & Blackwell, A. T. Detailed data for 259 fireballs from the Canadian camera network and inferences concerning the influx of large meteoroids. *Meteoritics* **31,** 185–217 (1996).
19. ReVelle, D. O. *Meteoroids 2001—Conference Proceedings* SP-495 (ed. Warmbein, B.) 483–498 (European Space Agency, Noordijuk, The Netherlands, 2001).
20. ReVelle, D. O. Historical detection of atmospheric impacts by large bolides using acoustic-gravity waves. *Ann. NY Acad. Sci.* **822,** 284–302 (1997).
21. Levison, H. F. *et al.* The mass disruption of Oort cloud comets. *Science* **296,** 2212–2215 (2002).
22. Borovicka, J. *et al.* The Moravka meteorite fall – III: Meteoroid initial size, history and composition. *Meteorit. Planet. Sci.* (submitted).
23. Brown, P. *et al.* An entry model for the Tagish Lake fireball using seismic, satellite and infrasound records. *Meteorit. Planet. Sci.* **37,** 661–675 (2002).
24. ReVelle, D. O., Whitaker, R. W., Armstrong, R. T.. *Proc. SPIE* **3434,** 66–77 (1998).
25. Brown, P. *et al.* The fall of the St Robert meteorite. *Meteorit. Planet. Sci.* **31,** 502–517 (1995).
26. Borovicka, J. & Spurný, P. Radiation study of two very bright terrestrial bolides and an application to the comet S–L 9 collision with Jupiter. *Icarus* **121,** 484–510 (1996).
27. Brown, P., Whitaker, R. W., ReVelle, D. O. & Tagliaferri, E. Multi-station infrasonic observations of two large bolides: signal interpretation and implications for monitoring of atmospheric explosions. *Geophys. Res. Lett.* **29,** 1–4 (2002).
28. Stewart, J. S. A near-Earth asteroid population estimate from the LINEAR survey. *Science* **294,** 1691–1693 (2001).
29. Morbidelli, A., Jedicke, R., Bottke, W. F., Michel, P. & Tedesco, E. F. From magnitudes to diameters: The albedo distribution of near-Earth objects and the Earth collision hazard. *Icarus* **158,** 329–343 (2002).

Acknowledgements We thank the US Department of Defense for making these data available. We also thank A.W. Harris, J. Borovicka and Z. Ceplecha for discussions; A.W. Harris for making available to us LINEAR debiased data before publication; and W. Bottke and R. Jedicke for comments and suggestions that improved an earlier version of this Letter. This work was supported in part by the Canada Research Chair program, and the Natural Sciences and Engineering Research Council of Canada. There is no implied endorsement by the U.S. Department of Defense of factual accuracy or opinion in this paper.

Competing interests statement The authors declare that they have no competing financial interests.

Correspondence and requests for materials should be addresses to P.B. (e-mail: pbrown@uwo.ca).